



**Soil gas  
geochemistry across  
fault zones**

X. Han et al.

This discussion paper is/has been under review for the journal Natural Hazards and Earth System Sciences (NHESS). Please refer to the corresponding final paper in NHESS if available.

# Rn and CO<sub>2</sub> geochemistry of soil gas across the active fault zones in the capital area of China

X. Han, Y. Li, J. Du, X. Zhou, C. Xie, and W. Zhang

CEA Key Laboratory of Earthquake Prediction (Institute of Earthquake Science, China Earthquake Administration), Beijing 100036, China

Received: 5 November 2013 – Accepted: 8 February 2014 – Published: 20 February 2014

Correspondence to: Y. Li (subduction6@hotmail.com)

Published by Copernicus Publications on behalf of the European Geosciences Union.

Title Page

Abstract

Introduction

Conclusions

References

Tables

Figures



Back

Close

Full Screen / Esc

Printer-friendly Version

Interactive Discussion



## Abstract

The present work is proposed to investigate the spatiotemporal variations of soil gas Rn and CO<sub>2</sub> across the active faults in the capital area of China, for the understanding of fault activities and the assessment of seismic hazard. A total of 342 soil gas sampling sites were measured twice in 2011 and 2012 along seven profiles across four faults. The results of soil gas surveys show that in each profile, due to the variation of gas emission rate, the concentrations of Rn and CO<sub>2</sub> changed in the vicinity of faults. Spatial distributions of Rn and CO<sub>2</sub> in the study areas were different from each other, which was attributed to soil types affecting the existence of Rn and CO<sub>2</sub>. Compared with 2011 soil gas survey, the increases of Rn and CO<sub>2</sub> concentrations in 2012 were related to the enhancement of seismic activities in the capital area of China. Our results indicate that special attention for seismic monitoring should be paid to Xinbaoan-Shacheng Fault and the north east segment of Tangshan Fault in the future.

## 1 Introduction

Soil-gas measurement has received much attention as an effective method to trace hidden faults (e.g., Al-Hilal and Al-Ali, 2010; Baubron et al., 2002; Ciotoli et al., 2007; Fu et al., 2005; Walia et al., 2010) and monitor seismic activities (e.g., Kumar et al., 2009; Toutain and Baubron, 1999; Walia et al., 2012; Yang et al., 2005). The stress/strain changes related to seismic activity may force crustal fluid to migrate up, especially along faults (King, 1986), therefore altering the geochemical characteristics of the faults. Active faults, which are composed of highly fractured rock materials, gouge and fluid, favor gas leaks from the solid earth (Baubron et al., 2002; Toutain and Baubron, 1999). Spatiotemporal variations of soil gases at fault zone may reflect the regional crustal stress/strain changes related to seismotectonic activity (Fu et al., 2008; Zhou et al., 2010). Lombardi and Voltattorni (2010) studied the geochemistry characteristics of soil Rn, He and CO<sub>2</sub> in active and inactive faults in two areas of Italy, and found

**NHESSD**

2, 1729–1757, 2014

### Soil gas geochemistry across fault zones

X. Han et al.

Title Page

Abstract

Introduction

Conclusions

References

Tables

Figures

◀

▶

◀

▶

Back

Close

Full Screen / Esc

Printer-friendly Version

Interactive Discussion



## Soil gas geochemistry across fault zones

X. Han et al.

Title Page

Abstract

Introduction

Conclusions

References

Tables

Figures

◀

▶

◀

▶

Back

Close

Full Screen / Esc

Printer-friendly Version

Interactive Discussion



the concentrations of soil gases were much higher in the Colpasquale (a seismically active region) than the Campidano Graben characterized by seismic quiescence, for seismic activity favoring gas migration from the deep. Before earthquakes, a sharp increase of soil Rn concentration in both sites, which are separately located in active and non-active tectonic zone of West Bengal, was reported by Ghosh et al. (2011), but the average radon concentration was much higher in the Jalpaiguri site located in active tectonic zone, compared to the Kolkata site with non-active tectonic zone. Camarda et al. (2012) analyzed the relationship between soil CO<sub>2</sub> emission and Mt Etna Volcano activity. The result implies that the anomalous degassing of CO<sub>2</sub> can be mainly controlled by migration of fresh magma from deep to shallow portions of the Etna plumbing system. Therefore, the enhanced tectonic activity favors the uprising of significant gas in the deep of the earth and consequently makes an increase in soil gas concentration.

The capital area of China (38.7 ~ 41.3° N, 114.1 ~ 119.9° E) is a densely populated and economically developed region, which consists of Beijing, Tianjin, Zhangjiakou and Tangshan, etc. Its seismicity mainly controlled by hidden active faults is high (Gao and Ma, 1993), particularly in Yanqing-Huailai basin, Sanhe-Pinggu and Tangshan regions. In Yanqing-Huailai basin, several earthquakes above  $M_S = 6.0$  once occurred, and 163 events above  $M_S = 2.0$  were recorded there from 1970 to 2004 (Zhu et al., 2006). In Sanhe-Pinggu region, four paleoearthquake events, including 1679  $M_S = 8.0$  Earthquake, have been identified that occurred within recent 20 000 yr and they showed quasi-periodic occurrence (Ran et al., 1997). In Tangshan area, the 1976  $M_S = 7.8$  Tangshan Earthquake occurred and caused 242 000 deaths in 1976 (State Seismological Bureau, 1982). As soil gases can be tracers for seismotectonic activities, soil gas investigations in the capital area of China are very important for the understanding of fault activities and the assessment of seismic hazard.

Soil gas surveys in the capital area have been carried out by some researchers since 1990s. The anomalies of soil gas CO<sub>2</sub> and H<sub>2</sub> was observed at Xiadian Fault before  $M_S = 4.8$  Haituoshan earthquake on 21 July 1990 and  $M_S = 5.8$  Guye earthquake on 23 July 1990, respectively (Gao and Fan, 1992). Lin et al. (1994) analyzed the relationship

## Soil gas geochemistry across fault zones

X. Han et al.

Title Page

Abstract

Introduction

Conclusions

References

Tables

Figures

◀

▶

◀

▶

Back

Close

Full Screen / Esc

Printer-friendly Version

Interactive Discussion



between  $H_2$  anomaly and the activity of Xiadian Fault, Tangshan Fault and Xianghe-Huangzhuang Fault.  $H_2$  was generated during the rupture of rock or water-rock reaction, which was related to the fault activity. Li et al. (2009) discussed the geochemical characteristics of soil gases in Yanqing-Huailai basin and found the concentrations of Rn,  $CO_2$ , He,  $H_2$  and Hg are higher in the east of the basin than the west, which may be related to the tectonic activity of the area. Li et al. (2013) investigated the concentrations of soil gases (Hg, Rn,  $H_2$ , He and  $CO_2$ ) in the Tangshan region, and identified that the gaseous anomalies are consistent with the trace of Tangshan Faults. Though soil gas investigations in the capital area have been made and some gratifying achievements have been obtained, the difference of fault activities in the capital area has been seldom systematically investigated by the tool of soil gas.

This work is proposed to study the spatiotemporal variations of soil gases across different faults in the capital area of China, for the understanding of fault activities and the assessment of seismic hazard from the measurements of soil gas Rn and  $CO_2$ .

## 2 Seismotectonic settings

The capital area is located in the north of Northern China. Its tectonic setting is complex that consists of Yanshan-Yinshan uplift, Taihang-Wutai uplift and North China Basin. The area is vulnerable by intense seismicity caused by numerous faults oriented in NE–SW direction (Xu et al., 2002). Low-velocity and high-conductivity anomalies, which may be related to fluids, were observed in the lower crust to the uppermost mantle below the foci of large earthquakes, such as 1976  $M_S = 7.8$  Tangshan Earthquake and the 1679  $M_S = 8.0$  Sanhe-Pinggu Earthquake (Huang and Zhao, 2004). Consequently, the seismogenic layer in the upper and middle crust may be weakened by the fluids in the lower crust, which may trigger large crustal earthquakes (Huang and Zhao, 2004).

## 2.1 Yanqing-Huailai basin

Yanqing-Huailai basin, including Yanqing-Fanshan sub-basin and Huailai-Zhuolu sub-basin, is located at the North China Plain and the northeastern edge of the Shanxi rift (Fig. 1a and b). The tectonic environment in the basin is complicated due to the coupling interaction between the Yinshan-Yanshan orogenic belt and the Shanxi rift. The North Edge Fault of Yanqing-Fanshan sub-basin (NEYF Fault), the largest active normal fault in Yanqing-Huailai basin, is 102 km in NE trend, dipping towards SE with a dip of 55–80° (Gao and Ma, 1993; Yu et al., 2004). Xinbaoan-Shacheng Fault intersecting with NEYF Fault is 26 km in 290° trend and dips towards SW from 65° to 75° (Gao and Ma, 1993). The earthquakes above  $M_S = 6.0$  occurred in the region, including 1337  $M_S = 6.5$  Langshan Earthquake and 1720  $M_S = 6.7$  Shacheng Earthquake (Earthquake Disaster Defense department of CEA, 1995; Fig. 1b).

The basements of Yanqing-Huailai basin are composed of Archaean metamorphic rocks, Proterozoic and Palaeozoic dolomites, gneisses and clastic rocks, interbedded with thin layers of coal as well as Mesozoic intermediate-basic to acid volcanics and pyroclastics. The Pliocene sediments mainly consist of grey cemented gravels, which were overlaid unconformably by the Pleistocene sediments, including fluvial and lacustrine sand, gravel, silt, and clay (Pavrides et al., 1999).

## 2.2 Xiadian Fault

The seismic area of the 1679  $M_S = 8.0$  Sanhe-Pinggu Earthquake is located at the intersection of Yinshan-Yanshan uplift and subsiding belt of the North China Plain (Zhang et al., 2002; Fig. 1c). Xiadian Fault, seismogenic structure of the 1679 Earthquake, is an important buried faults in the north of North China Plain, dipping in the range 50–70° with a NE strike (Xu et al., 2000). The Quaternary strata in Sanhe-Pinggu region are mainly composed of clay, sand, and aleurite (Jang et al., 2000).

**NHESSD**

2, 1729–1757, 2014

### Soil gas geochemistry across fault zones

X. Han et al.

Title Page

Abstract

Introduction

Conclusions

References

Tables

Figures

◀

▶

◀

▶

Back

Close

Full Screen / Esc

Printer-friendly Version

Interactive Discussion



## 2.3 Tangshan Fault

Tangshan region close to the north of the North China Plain and located at the southern edge of Yanshan uplift is known as a “rhombic block” surrounded by four large faults (Fig. 1a). Tangshan Fault, seismogenic structure of 1976  $M_S = 7.8$  Tangshan Earthquake, located along the diagonal of the “rhombic block”, consists of several NE strike segments with high dip angles and right-lateral slip (Fig. 1d). A fault slip rate of  $2.6 \text{ mm yr}^{-1}$  at 15 km depth was obtained from the analysis of the repeating of seismic events observed along the Tangshan Fault (Li et al., 2007).

## 3 Methodology

Rn and  $\text{CO}_2$  were sampled by inserting a hollow stainless steel sampler of 3 cm diameter into the ground to a depth of 80 cm. The sampler was connected to radon detector through rubber tubes. Radon measurement was performed in the field using a radon detector RAD7. The working principle is counting the  $\alpha$ -particles emitted during the decay of  $^{222}\text{Rn}$  to  $^{218}\text{Po}$ . It takes 15 min for radon analysis at each sampling site. The sensitivity and measurement error of the radon detector are  $14.8 \text{ Bqm}^{-3}$  and  $\pm 5\%$ , respectively (Zhou et al., 2010). Soil gas  $\text{CO}_2$  was analyzed by using an Agilent 3000 gas chromatography (GC) by means of a thermal conductivity detector (TCD) with a measurement error of  $\pm 5\%$ . Soil gas  $\text{CO}_2$  sampled from the sampling device were injected immediately into the GC by a glass syringe. The detection limit of  $\text{CO}_2$  is 2 ppm (Li et al., 2009).

Soil gas surveys were carried out twice during August to September 2011 and September to October 2012. Meteorological parameters, such as temperature, atmospheric pressure, wind, precipitation and air moisture, varied slightly between the two times soil gas surveys (Fig. 2). The soil gases were sampled along the measuring line at a distance of 20 m, and the distance between two parallel measuring lines is 5 m. In Yanqing-Huailai basin, 50 and 33 sampling sites of soil gases were measured

## Soil gas geochemistry across fault zones

X. Han et al.

Title Page

Abstract

Introduction

Conclusions

References

Tables

Figures

◀

▶

◀

▶

Back

Close

Full Screen / Esc

Printer-friendly Version

Interactive Discussion





values, except Rn at PG profile in 2011 and LY profile in 2012 and CO<sub>2</sub> at PG profile in 2011, DG profile in 2011 and FN profile in 2011, obey normal distribution (sig.< 0.05 in Kolmogorov–Smirnov test).

Figure 3 shows the distributions of Rn and CO<sub>2</sub> along two parallel measuring lines LYI and LYII (5 m between the two parallel measuring lines) across the NEYF Fault. In LY profile, Rn varies from 2.4 to 13.2 kBqm<sup>-3</sup> and from 1.7 to 19.1 kBqm<sup>-3</sup> in 2011 and 2012 soil gas surveys, respectively; CO<sub>2</sub> ranges from 806.0 to 10 345.0 ppm and from 1005.3 to 21 697.8 ppm in 2011 and 2012 soil gas surveys, respectively. Anomalously high concentrations of Rn and CO<sub>2</sub> along the two measuring lines can be found near the NEYF fault (Fig. 3). However, both Rn and CO<sub>2</sub> did not present high concentrations on the fault, which may imply the fault contains gouge and ultracataclasite with a low permeability. Spatial distributions of Rn and CO<sub>2</sub> along the two profiles show that the increase of CO<sub>2</sub> during the period of soil gas investigations was greater than Rn (Fig. 3).

The measuring results of Rn and CO<sub>2</sub> along DY profile show that Rn and CO<sub>2</sub> concentrations increased sharply in 2012 compared with 2011, especially from 320 to 640 m along the profile, which was located on the hanging wall of the fault (Fig. 4). The variations of Rn and CO<sub>2</sub> are attributed to the geological factors, especially the fault activity.

In Sanhe-Pinggu region, Rn and CO<sub>2</sub> were sampled along three profiles across Xiadian fault (Fig. 1c). In the two times soil gas surveys, the average concentration of CO<sub>2</sub> at QX, PG and DG profiles varies from 6828.2 to 11 467.2 ppm, 6123.0 to 10 273.1 ppm and 5609.6 to 12 119.9 ppm, respectively; the average concentration of Rn at QX, PG and DG profiles ranges from 10.4 to 16.0 kBqm<sup>-3</sup>, 20.2 to 26.3 kBqm<sup>-3</sup> and 12.4 to 27.7 kBqm<sup>-3</sup>, respectively. It can be noted that the concentrations of CO<sub>2</sub> and Rn both increased at these profiles, but the increase of CO<sub>2</sub> and Rn at DG profile is greater than QX and PG profiles, particularly the increase of Rn. It indicates that variations of Rn and CO<sub>2</sub> may be caused by regional crustal stress/strain changes. The inhomogeneous leakage of Rn and CO<sub>2</sub> occur on the Xiadian Fault (Figs. 5, 6 and 7).

## Soil gas geochemistry across fault zones

X. Han et al.

Title Page

Abstract

Introduction

Conclusions

References

Tables

Figures

◀

▶

◀

▶

Back

Close

Full Screen / Esc

Printer-friendly Version

Interactive Discussion



## Soil gas geochemistry across fault zones

X. Han et al.

Title Page	
Abstract	Introduction
Conclusions	References
Tables	Figures
⏪	⏩
◀	▶
Back	Close
Full Screen / Esc	
Printer-friendly Version	
Interactive Discussion	



The sampling sites with anomalously high concentrations of soil gas were located at isolated points known as gas vents on the Xiadian Fault, but the ones with low concentrations were located at low permeability zones on the fault (Annunziatellis et al., 2008). It implies inhomogeneous leakage caused by permeability heterogeneity along the Xiadian Fault zone. At some sampling sites, the anomalous concentrations of Rn and CO<sub>2</sub> do not always synchronize with each other. It suggests the source of Rn and CO<sub>2</sub> at the sampling site for deep source component with high values of Rn and CO<sub>2</sub> and shallow source component with high CO<sub>2</sub> but low Rn concentrations.

Figure 8 shows the distributions of Rn and CO<sub>2</sub> along GY profile across the Tangshan Fault. In the two times soil gas investigations, the maximum concentrations of Rn and CO<sub>2</sub> at GY profile increased from 18.5 to 34.6 kBq m<sup>-3</sup> and 10 706.2 to 40 315.5 ppm, respectively. The anomalies of Rn and CO<sub>2</sub> along GY profile in 2012 soil gas survey present irregular shapes. It may be related to the seismicity in Tangshan region, which will be discussed in later section. Spatial distributions of Rn and CO<sub>2</sub> along the profile FN show double peak anomalies (Fig. 9), which implied that Tangshan Faults were mature faults with fault cores and damage zones (Annunziatellis et al., 2008). Fault cores composed of gouge and ultracataclasite with a low permeability prevent gas migration from deep to surface, but the damage zones with high permeability favor the uprising of deep sourced gases (Faulkner et al., 2010; Annunziatellis et al., 2008). Compared with soil gas survey in 2011, the concentrations of Rn along profile FN changed slightly but the concentrations of CO<sub>2</sub> were increased in 2012.

### 4.2 Fault activities

The concentrations of soil gas can be affected by seismotectonic activity, rock types, porosity and composition of soil, meteorological parameters (e.g. Temperature, precipitation and air moisture, etc.) and structural type (Fu et al., 2005, 2008; Hink, 1994; Lombardi and Voltattorni, 2010; Toutain and Baubron, 1999; Walia et al., 2008; Zhou et al., 2010). As meteorological parameters varied slightly between the two times soil gas surveys (Fig. 2), the concentration variations of Rn and CO<sub>2</sub> at the same sampling

site were mainly controlled by stress/strain changes related to seismotectonic activity. In order to compare the activities of faults in the study area, the average concentration ratio (ACR) and maximum concentration ratio (MCR) of soil gas were proposed to avoid the other factors influencing the gas concentrations. ACR and MCR can be calculated by the following Eq. (1) and Eq. (2):

$$ACR = {}^{2012}Q_{aver.} / {}^{2011}Q_{aver.} \quad (1)$$

where  ${}^{2012}Q_{aver.}$  is the average concentration of soil gas at one profile in 2012, and  ${}^{2011}Q_{aver.}$  is the average concentration of soil gas at corresponding profile in 2011;

$$MCR = {}^{2012}Q_{max} / {}^{2011}Q_{max} \quad (2)$$

where  ${}^{2012}Q_{max}$  is the maximum concentration of soil gas at one profile in 2012, and  ${}^{2011}Q_{max}$  is the maximum concentration of soil gas at corresponding profile in 2011.

The ACRs and MCRs of Rn and CO<sub>2</sub> are illustrated in Fig. 10a. The ACRs of Rn and CO<sub>2</sub> at DY and DG profiles are greater than 2.0; the MCRs of Rn and CO<sub>2</sub> at GY profile are greater than the other profiles. As the ACRs and MCRs of Rn and CO<sub>2</sub> at DY profile are greater than LY profile, it may imply that the activity of Xinbaoan-Shacheng Fault is more intense than NEYF Fault. The ACRs and MCRs of Rn and CO<sub>2</sub> at QX and PG profiles are less than that at DG profiles, which may indicate that the south segment of Xiadian Faults is more active than the middle segment. As the ACRs and MCRs of Rn and CO<sub>2</sub> at GY profile are greater than FN profile, it may suggest the activity of the north east segment of Tangshan Fault is more intense than the south west segment.

The anomaly thresholds of Rn and CO<sub>2</sub> have increased at different levels in the second time soil gas survey (Fig. 10b), which may imply the seismic activities in the Capital area has been enhanced. Based on the data from China Earthquake Networks Center, there were 131 earthquakes ( $M_S \geq 1.8$ ) recorded in the Capital area in 2011, but 221 earthquakes ( $M_S \geq 1.8$ ) were recorded in 2012. Figure 1a shows the locations of earthquakes ( $M_S \geq 3.0$ ) in Capital area since 1 January 2011. There was no earthquake ( $M_S \geq 3.0$ ) reported in Capital area from 1 January 2011 to 1 December 2011.

**Soil gas  
geochemistry across  
fault zones**

X. Han et al.

Title Page

Abstract

Introduction

Conclusions

References

Tables

Figures



Back

Close

Full Screen / Esc

Printer-friendly Version

Interactive Discussion



However, it has been recorded 5 earthquakes ( $M_S \geq 3.0$ ) in 2012. These evidences enabled us to confirm the inference from our results. The permeability of pathways increased by the enhanced seismic activities, resulting in more significant gas migrates to the surface (Lombardi and Voltattorni, 2010).

The seismic activity in the north east segment of Tangshan Faults is more intense than the south west segment, for the evidence that 99 earthquakes ( $M_S \geq 1.8$ ) occurred on the north east segment during the period of 2011 and 2012, compared with that 15 earthquakes ( $M_S \geq 1.8$ ) happened on the south west segment. It may coincide with the inference from the results of soil gas surveys in Tangshan region. The irregularly shaped diffuse anomalies of Rn and  $\text{CO}_2$  along the profile GY in 2012 soil gas survey may be related to the  $M_S = 4.7$  earthquake (28 May 2012) and the  $M_S = 3.7$  earthquake (29 May 2012) (Fig. 1a). New fractures were formed by the two seismic events and the structures became more permeable, resulting in the increase of Rn and  $\text{CO}_2$  concentrations.

### 4.3 The difference of spatial distributions in the study areas

The concentrations of Rn in Sanhe-Pinggu region, Tangshan region and Yanqing-Huailai basin showed a decending tendency (Fig. 10c). The concentrations of Rn in Yanqing-Huailai basin should be higher compared with Sanhe-Pinggu and Tangshan regions, as the basements of Yanqing-Huailai basin contain acid volcanics and pyroclastics (Pavlidis et al., 1999). However, the values of Rn at DY and LY profiles were not higher, even lower than Sanhe-Pinggu and Tangshan regions. The greater porosity of sandy soil (Table 2) and less precipitation (Fig. 2) in Yanqing-Huailai basin favor gas exchange between soil gas and air. The soil with greater porosity could present lower Rn values for dilution by atmospheric air (Fu et al., 2005). Less rainfall could decrease the moisture content of soil and rock, such decreasing the emanation of Rn to migrate into soil pore (King, 1986). Furthermore, as crustal thickness in Yanqing-Huailai basin is larger than the other two regions (Wang et al., 2009), the soil gas at DY and LY profiles would contain less deep gas of Rn for the decay of  $^{222}\text{Rn}$  to  $^{218}\text{Po}$  with migration.

## Soil gas geochemistry across fault zones

X. Han et al.

Title Page

Abstract

Introduction

Conclusions

References

Tables

Figures

◀

▶

◀

▶

Back

Close

Full Screen / Esc

Printer-friendly Version

Interactive Discussion



Compared with Sanhe-Pinggu region, lower values of Rn in Tangshan is affected by the high soil moisture attributed to the low ground water level (Li et al., 2013). The emanation coefficient of Rn will decrease when the moisture content of soil increases and reaches saturated conditions (Menetrez and Mosley, 1996).

However, the soil CO<sub>2</sub> accumulation in Yanqing-Huailai basin, Sanhe-Pinggu region and Tangshan region is different from Rn (Fig. 10c). The average concentrations of CO<sub>2</sub> in study areas have a little difference except CO<sub>2</sub> at DY(2012) profile, where aseismic fault slip may cause a sharp increase on the concentrations of CO<sub>2</sub> (Fig. 10c). This phenomenon may be attributed to different soil types in study areas (Table 2). Gal et al. (2011) studied the relationship between soil gas behavior and soil types, and discovered that coarse grained soils can be benefit for the existence of CO<sub>2</sub>, but fine grained clayey soils are in favor of the existence of Rn. Both topsoil and subsoil at DY profile are sand with higher permeability, which favors the gas exchange between soil gas and air. However, the average values of CO<sub>2</sub> in DY profile are a little higher than the other profiles due to the oxidation of soil organic carbon (SOC) with higher content (Table 2). The decomposition rate of organic material in soil is equal to the supply rate under natural condition, and the content of organic material in soil is constant (Buringh, 1984). The more CO<sub>2</sub> could release into the soil pore as SOC with higher content is oxidated. In other profiles, the average concentrations of CO<sub>2</sub> have a little difference for different soil types, although the content of SOC and the fraction of sand, silt and clay in soil are similar with each other.

## 5 Conclusions

The spatiotemporal variations of Rn and CO<sub>2</sub> in soil gas in seismically active areas, the capital area of China, were studied based on the two times soil gas surveys at 342 sampling sites. As meteorological parameters varied slightly between the two times soil gas surveys, a sharp increase in Rn and CO<sub>2</sub> concentrations at the same sampling site was mainly controlled by stress/strain redistribution related to seismotectonic activity.

## Soil gas geochemistry across fault zones

X. Han et al.

Title Page

Abstract

Introduction

Conclusions

References

Tables

Figures

⏪

⏩

◀

▶

Back

Close

Full Screen / Esc

Printer-friendly Version

Interactive Discussion



The increases of Rn and CO<sub>2</sub> concentrations in 2012 soil gas survey may be related to the enhancement of seismic activities in the capital area of China. Based on the average and maximum concentration ratios of Rn and CO<sub>2</sub> between the two times soil gas surveys, it can be inferred that the activities of Xinbaoan-Shacheng Fault and the north east segment of Tangshan Fault are more intense and they should be paid particular attention for seismic hazard in the future. Furthermore, soil type may play an important role in the concentration of different significant gases.

*Acknowledgements.* This work was financially supported by the Basic Research Project of Institute of Earthquake Science, CEA (02132420, 0213241503). The authors would like to thank Xiaoqiang Li for his help in sample collecting and measurement.

## References

- Al-Hilal, M. and Al-Ali, A.: The role of soil gas radon survey in exploring unknown subsurface faults at Afamia B dam, Syria, *Radiat. Meas.*, 45, 219–224, 2010.
- Annunziatellis, A., Beaubien, S. E., Bigi, S., Ciotoli, G., Coltella, M., and Lombardi, S.: Gas migration along fault systems and through the vadose zone in the Latera caldera (central Italy): implications for CO<sub>2</sub> geological storage, *Int. J. Greenh. Gas Con.*, 2, 353–372, 2008.
- Baubron, J. C., Rigo, A., and Toutain, J. P.: Soil gas profiles as a tool to characterize active tectonic areas: the Jaut Pass example (Pyrenees, France), *Earth. Planet. Sc. Lett.*, 196, 69–81, 2002.
- Buringh, P.: Organic carbon in soils of the world, the role of terrestrial vegetation in the global carbon cycle, measurement by remote sensing, *SCOPE Ser.*, 23, 91–109, 1984.
- Camarda, M., De Gregorio, S., and Gurrieri, S.: Magma-ascent processes during 2005–2009 at Mt Etna inferred by soil CO<sub>2</sub> emissions in peripheral areas of the volcano, *Chem. Geol.*, 330–331, 218–227, 2012.
- Ciotoli, G., Guerra, M., Lombardi, E., and Vittori, E.: Soil gas survey for tracing seismogenic faults: a case study in the Fucino basin, Central Italy, *J. Geophys. Res.*, 103, 23781–23794, 1998.

## Soil gas geochemistry across fault zones

X. Han et al.

Title Page

Abstract

Introduction

Conclusions

References

Tables

Figures

⏪

⏩

◀

▶

Back

Close

Full Screen / Esc

Printer-friendly Version

Interactive Discussion



## Soil gas geochemistry across fault zones

X. Han et al.

Title Page

Abstract

Introduction

Conclusions

References

Tables

Figures

◀

▶

◀

▶

Back

Close

Full Screen / Esc

Printer-friendly Version

Interactive Discussion



Ciotoli, G., Lombardi, S., and Annunziatellis, A.: Geostatistical analysis of soil gas data in a high seismic intermontane basin: Fucino Plain, central Italy, *J. Geophys. Res.*, 112, B05407, doi:10.1029/2005JB004044, 2007.

Earthquake Disaster Defense department of CEA: Chinese historical strong earthquake catalog (The 23rd century BC-1911 AD), Seismological Press, Beijing, 1995 (in Chinese).

FAO/IIASA/ISRIC/ISSCAS/JRC: Harmonized World Soil Database (version 1.2), FAO, Rome, Italy and IIASA, Laxenburg, Austria, 2012.

Faulkner, D. R., Jackson, C. A. L., Lunn, R. J., Schlische, R. W., Shipton, Z. K., Wibberley, C. A. J., and Withjack, M. O.: A review of recent developments concerning the structure, mechanics and fluid flow properties of fault zones, *J. Struct. Geol.*, 32, 1557–1575, 2010.

Fu, C. C., Yang, T. F., Walia, V., and Chen, C. H.: Reconnaissance of soil gas composition over the buried fault and fracture zone in southern Taiwan, *Geochem. J.*, 39, 427–439, 2005.

Fu, C. C., Yang, T. F., Du, J., Walia, V., Chen, Y. G., Liu, T. K., and Chen, C. H.: Variations of helium and radon concentrations in soil gases from an active fault zone in southern Taiwan, *Radiat. Meas.*, 43, S348–S352, 2008.

Gal, F., Joubin, F., Haas, H., Jean-prost, V., and Ruffier, V.: Soil gas ( $^{222}\text{Rn}$ ,  $\text{CO}_2$ ,  $^4\text{He}$ ) behaviour over a natural  $\text{CO}_2$  accumulation, Montmiral area (Drôme, France): geographical, geological and temporal relationships, *J. Environ. Radioact.*, 102, 107–118, 2011.

Gao, Q. W. and Fan, S. Q.: The anomalies of Fault gas reflected by Xiadian Faults before the earthquake, *Earthq.*, 12, 73–76, 1992 (in Chinese).

Gao, W. X. and Ma, J.: Seismic Geological Environment and Seismic Hazard in the Capital Area, Seismological Press, Beijing, 1993 (in Chinese).

Ghosh, D., Deb, A., Sengupta, R., Bera, S., Sahoo, S. R., Haldar, S., and Patra, K. K.: Comparative study of seismic surveillance on radon in active and non-active tectonic zone of West Bengal, India, *Radiat. Meas.*, 46, 365–370, 2011.

Guo, H., Jiang, W. L., and Xie, X. S.: Late-Quaternary strong earthquakes on the seismogenic fault of the 1976 Ms7.8 Tangshan earthquake, Hebei, as revealed by drilling and trenching, *Sci. China Earth Sci.*, 54, 1696–1715, doi:10.1007/s11430-011-4218-x, 2011.

Hinkle, M. E.: Environmental conditions affecting concentrations of He,  $\text{CO}_2$ ,  $\text{O}_2$  and  $\text{N}_2$  in soil gases, *Appl. Geochem.*, 9, 53–63, 1994.

Huang, J. L. and Zhao, D. P.: Crustal heterogeneity and seismotectonics of the region around Beijing, China, *Tectonophysics*, 385, 159–180, 2004.

## Soil gas geochemistry across fault zones

X. Han et al.

Title Page

Abstract

Introduction

Conclusions

References

Tables

Figures

◀

▶

◀

▶

Back

Close

Full Screen / Esc

Printer-friendly Version

Interactive Discussion



- Jiang, W. L., Hou, Z. H., Xiao, Z. M., and Xie, X. S.: Study on Paleoearthquakes of Qixinzhuang trench at the Xiadian Fault, Beijing plain, *Seism. Geol.*, 22, 413–422, 2000 (in Chinese).
- King, C. Y.: Gas geochemistry applied to earthquake prediction: an overview, *J. Geophys. Res.*, 91, 12269–12281, 1986.
- 5 Kumar, A., Singh, S., Mahajan, S., Bajwa, B. S., Kalia, R., and Dhar, S.: Earthquake precursory studies in Kangra valley of North West Himalayas, India, with special emphasis on radon emission, *Appl. Radiat. Isot.*, 67, 1904–1911, 2009.
- Li, L., Chen, Q. F., Cheng, X., and Niu, F. L.: Spatial clustering and repeating of seismic events observed along the 1976 Tangshan fault, north China, *Geophys. Res. Lett.*, 34, L23309, doi:10.1029/2007GL031594, 2007.
- 10 Li, Y., Du, J. G., Wang, F. K., Zhou, X. C., Pan, X. D., and Wei, R. Q.: Geochemical characteristics of soil gas in the Yanhuai basin, northern China, *Earthq. Sci.*, 22, 93–100, 2009.
- Li, Y., Du, J. G., Wang, X., Zhou, X. C., Xie, C., and Cui, Y. J.: Spatial variations of soil gas geochemistry in the Tangshan area, Northern China, *Terr. Atmos. Ocean Sci.*, 24, 323–332, 2013, <http://www.ocean-sci.net/24/323/2013/>.
- 15 Lin, Y. W., Zhai, S. H., Fan, S. Q., and Kong, L. C.: Study on characteristic and mechanism of H<sub>2</sub> anomaly on the hidden active faults in north China, *Seism. Geol.*, 16, 264–268, 1994 (in Chinese).
- 20 Lombardi, S. and Voltattorni, N.: Rn, He and CO<sub>2</sub> soil gas geochemistry for the study of active and inactive faults, *Appl. Geochem.*, 25, 1206–1220, 2010.
- Menetrez, M. Y. and Mosley, R. B.: Evaluation of radon emanation from soil with varying moisture content in a soil chamber, *Environ. Int.*, 22, Suppl. 1, S447–S453, 1996.
- Pavlidis, S. B., Zouros, N. C., Fang, Z. J., Cheng, S. P., Tranos, M. D., and Chatzipetros, A. A.: Geometry, kinematics and morphotectonics of the Yanqing-huilai active faults (Northern China), *Tectonophysics*, 308, 99–118, 1999.
- 25 Ran, Y. K., Deng, Q. D., Yang, X. P., Zhang, W. X., Li, R. C., and Xiang, H. F.: Paleoearthquakes and recurrence interval on the seismogenic fault of 1679 Sanhe-Pinggu Ms 8.0 earthquake Hebei and Beijing, *Seism. Geol.*, 19, 193–201, 1997 (in Chinese).
- 30 Seismic Geological Brigade, China Earthquake Administration: The systematic active tectonic map in Beijing area, China printing plant, Shanghai, 1979 (in Chinese).
- Seminsky, K. Zh., and Demberel, S.: The first estimations of soil-radon activity near faults in Central Mongolia, *Radiat. Meas.*, 49, 19–34, 2013.

## Soil gas geochemistry across fault zones

X. Han et al.

Title Page

Abstract

Introduction

Conclusions

References

Tables

Figures

◀

▶

◀

▶

Back

Close

Full Screen / Esc

Printer-friendly Version

Interactive Discussion



- State Seismological Bureau: Tangshan earthquake of 1976, Seismology Publisher, Beijing, 1982 (in Chinese).
- Toutain, J. P. and Baubron, J. C.: Gas geochemistry and seismotectonics: a review, *Tectonophysics*, 304, 1–27, 1999.
- 5 Walia, V., Mahajan, S., Kumar, A., Singh, S., Bajwa, D. S., Dhar, S., and Yang, T. F.: Fault delineation study using soil-gas method in the Dharamsala area, NW Himalayas, India, *Radiat. Meas.*, 43, S337–S342, 2008.
- Walia, V., Lin, S. J., Fu, C. C., Yang, T. F., Hong, W. L., Wen, K. L., and Chen, C. H.: Soil-gas monitoring: A tool for fault delineation studies along Hsinhua Fault (Tainan), Southern  
10 Taiwan, *Appl. Geochem.*, 25, 602–607, 2010.
- Walia, V., Yang, T. F., Lin, S. J., Kumar, A., Fu, C. C., Chiu, J. M., Chang, H. H., Wen, K. L., and Chen, C. H.: Temporal variation of soil gas compositions for earthquake surveillance in Taiwan, *Radiat. Meas.*, 50, 154–159, doi:10.1016/j.radmeas.2012.11.007, 2012.
- 15 Wang, J., Liu, Q. Y., Chen, J. H., Li, S. C., Guo, B., and Li, Y.: The crustal thickness and Poisson's ratio beneath the Capital Circle Region, Chin. *J. Geophys.*, 52, 57–66, 2009 (in Chinese).
- Xu, X. W., Ji, F. J., Yu, G. H., Chen, W. B., Wang, F., and Jiang, W. L.: Reconstruction of paleoearthquake sequence using stratigraphic records from drill logs: a study at the Xiadian Fault, Beijing, *Seism. Geol.*, 22, 9–19, 2000 (in Chinese).
- 20 Xu, X. W., Wu, W. M., Zhang, X. K., Ma, S. L., Ma, W. T., Yu, G. H., Gu, M. L., and Jiang, W. L.: New Crustal Structure Motion and Earthquake in Capital Area, Science Press, Beijing, 2002 (in Chinese).
- Yang, T. F., Walia, V., Chyi, L. L., Fu, C. C., Chen, C. H., Liu, T. K., Song, S. R., Lee, C. Y., and Lee, M.: Variations of soil radon and thoron concentrations in a fault zone and prospective  
25 earthquakes in SW Taiwan, *Radiat. Meas.*, 40, 496–502, 2005.
- Yin, B. J.: Dynamic characteristics of underground water in the Tangshan well, Ph. D. thesis, Institute of Geophysics, China Earthquake Administration, China, 37 pp., 2010 (in Chinese).
- Yu, G. H., Xu, X. W., Ma, W. T., Zhu, A. L., Diao, G. L., Zhang, S. C., Zhang, X. K., Liu, B. J., and Sun, Z. G.: Study on relationship between deep and shallow structures along north boundary  
30 fault of Yanqing-Fanshan basin, *Acta Seism. Sinica*, 26, 68–76, 2004 (in Chinese).
- Zhang, X. K., Zhao, J. R., Liu, G. H., Song, W. R., Liu, B. J., Zhao, C. B., Cheng, S. X., Liu, J. D., Gu, M. L., and Sun, Z. G.: Study on fine crustal structure of the Sanhe-Pinggu Earthquake

(M8.0) region by deep seismic reflection profiling, Earthq. Res. China, 18, 326–336, 2002 (in Chinese).

Zhou, X. C., Du, J. G., Chen, Z., Cheng, J. W., Tang, Y., Yang, L. M., Xie, C., Cui, Y. J., Liu, L., Yi, L., Yang, P. X., and Li, Y.: Geochemistry of soil gas in the seismic fault zone produced by the Wenchuan Ms 8.0 earthquake, southwestern China, Geochem. Trans., 11, doi:10.1186/1467-4866-11-5, 2010.

Zhu, H. S., Zhao, C. M., Li, G. H., Xue, Z. F., and Jiang, W.: Tectonic characteristics of Yanhuai basin and evaluation of potential seismic risk, North. China, Earthq. Sci., 24, 38–42, 2006 (in Chinese).

# NHESSD

2, 1729–1757, 2014

## Soil gas geochemistry across fault zones

X. Han et al.

Title Page

Abstract

Introduction

Conclusions

References

Tables

Figures

◀

▶

◀

▶

Back

Close

Full Screen / Esc

Printer-friendly Version

Interactive Discussion



## Soil gas geochemistry across fault zones

X. Han et al.

**Table 1.** Main statistical parameters of soil gas surveys in capital area of China.

Area	Profiles	Gas	Samples	2011					2012						
				Min	Max	Mean	Median	SD	Anomaly threshold	Min	Max	Mean	Median	SD	Anomaly threshold
Yanqing-Huailai basin	LY	CO <sub>2</sub> (ppm)	50	806.0	10 345.0	4277.9	3784.3	2300.5	6578.4	1005.3	21697.8	7235.3	6300.1	3992.2	11 227.5
	LY	Rn (kBq m <sup>-3</sup> )	50	2.4	13.2	5.9	5.7	2.1	8.0	1.7	19.1	7.8	7.6	2.9	9.8
	DY	CO <sub>2</sub> (ppm)	33	1477.7	14 505.0	7715.2	7412.7	3035.1	10 750.3	6480.7	39 304.8	17 875.0	17 254.7	8118.6	25 993.6
	DY	Rn (kBq m <sup>-3</sup> )	33	0.8	6.5	2.9	2.7	1.2	4.1	1.0	11.1	5.9	5.9	2.1	8.0
Sanhe-pinggu region	QX	CO <sub>2</sub> (ppm)	66	957.0	19 414.5	6828.2	6221.0	3724.6	10 552.8	6133.9	17 279.0	11 467.2	11 344.8	2263.6	13 730.8
	QX	Rn (kBq m <sup>-3</sup> )	66	2.4	24.1	10.4	9.2	5.4	15.8	5.4	28.7	16.0	15.7	5.1	21.1
	PG	CO <sub>2</sub> (ppm)	72	821.8	30 616.5	6123.0	4352.1	5506.0	9342.9	2982.7	26 314.1	10 273.1	9988.9	4429.4	14 702.5
	PG	Rn (kBq m <sup>-3</sup> )	72	1.9	71.1	20.2	15.6	16.0	32.7	6.2	61.4	26.3	25.0	12.4	38.7
	DG	CO <sub>2</sub> (ppm)	50	688.5	23 524.5	5609.6	4436.2	4962.8	9196.7	2089.2	27 110.6	12 119.9	11 632.0	5500.2	17 620.1
	DG	Rn (kBq m <sup>-3</sup> )	50	2.9	43.1	12.4	10.6	8.2	20.6	5.4	58.0	27.7	26.7	10.5	38.2
Tangshan region	GY	CO <sub>2</sub> (ppm)	48	2624.0	10 706.2	6690.8	6902.4	2379.6	9070.4	453.2	40 315.5	13 225.8	12 285.3	11 091.0	24 316.8
	GY	Rn (kBq m <sup>-3</sup> )	48	0.9	18.5	6.6	5.3	3.8	10.4	0.7	34.6	11.5	11.6	7.8	19.3
	FN	CO <sub>2</sub> (ppm)	23	522.0	66 317.0	5652.9	1998.7	13 631.7	6434.8	517.1	30 853.6	9402.6	7455.5	9031.3	18 433.9
	FN	Rn (kBq m <sup>-3</sup> )	23	1.0	20.3	5.5	2.7	5.9	11.4	0.9	20.5	8.5	7.5	6.9	15.4

Title Page

Abstract

Introduction

Conclusions

References

Tables

Figures

◀

▶

◀

▶

Back

Close

Full Screen / Esc

Printer-friendly Version

Interactive Discussion



## Soil gas geochemistry across fault zones

X. Han et al.

**Table 2.** Component percentages in soil in the study areas (FAO/IIASA/ISRIC/ISSCAS/JRC, 2012).

Profile	Soil unit Name (FAO 90)	Topsoil (0–30 cm)					USDA Texture Classification	Subsoil (30–100 cm)					USDA Texture Classification
		Sand Fraction (%)	Silt Fraction (%)	Clay Fraction (%)	Gravel Content (%)	Organic Carbon (% weight)		Sand Fraction (%)	Silt Fraction (%)	Clay Fraction (%)	Gravel Content (%)	Organic Carbon (% weight)	
LY	Salic Fluvisols	37	46	17	4	0.42	loam	37	42	21	8	0.47	loam
DY	Cumulic Anthrosols	90	6	4	10	2.41	sand	89	6	5	10	0.88	sand
QX	Calcaric Cambisols	36	43	21	6	0.65	loam	34	43	23	10	0.43	loam
PG	Calcaric Cambisols	36	43	21	6	0.65	loam	34	43	23	10	0.43	loam
DG	Calcaric Cambisols	36	43	21	6	0.65	loam	34	43	23	10	0.43	loam
GY	Gleyic Luvisols	47	29	24	5	0.83	loam	39	27	34	6	0.28	clay loam
FN	Calcic Gleysols	41	40	19	4	1.3	loam	44	37	19	5	0.44	loam

Title Page

Abstract

Introduction

Conclusions

References

Tables

Figures

⏪

⏩

◀

▶

Back

Close

Full Screen / Esc

Printer-friendly Version

Interactive Discussion



## Soil gas geochemistry across fault zones

X. Han et al.

Title Page

Abstract

Introduction

Conclusions

References

Tables

Figures

◀

▶

◀

▶

Back

Close

Full Screen / Esc

Printer-friendly Version

Interactive Discussion

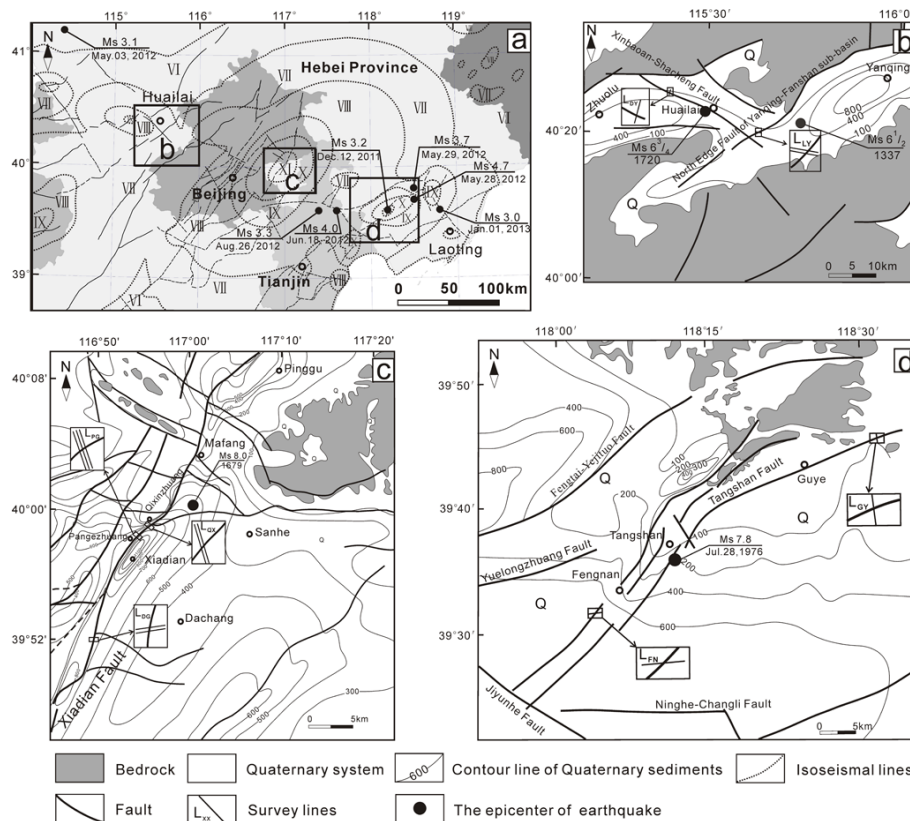


**Fig. 1.** Simplified geological maps of study areas in the capital area of China (modified after Zhu et al., 2006; Seismic Geological Brigade, CEA, 1979; Yin, 2010; Guo et al., 2011). **(a)** shows the locations of study areas and locations of earthquakes ( $M_S \geq 3.0$ ) occurring in the capital area from 1 January 2011 to 1 January 2013. **(b–d)** show the geologic structure and locations of soil gas profiles in Yanqing-Huailai basin, Sanhe-Pinggu and Tangshan regions, respectively.

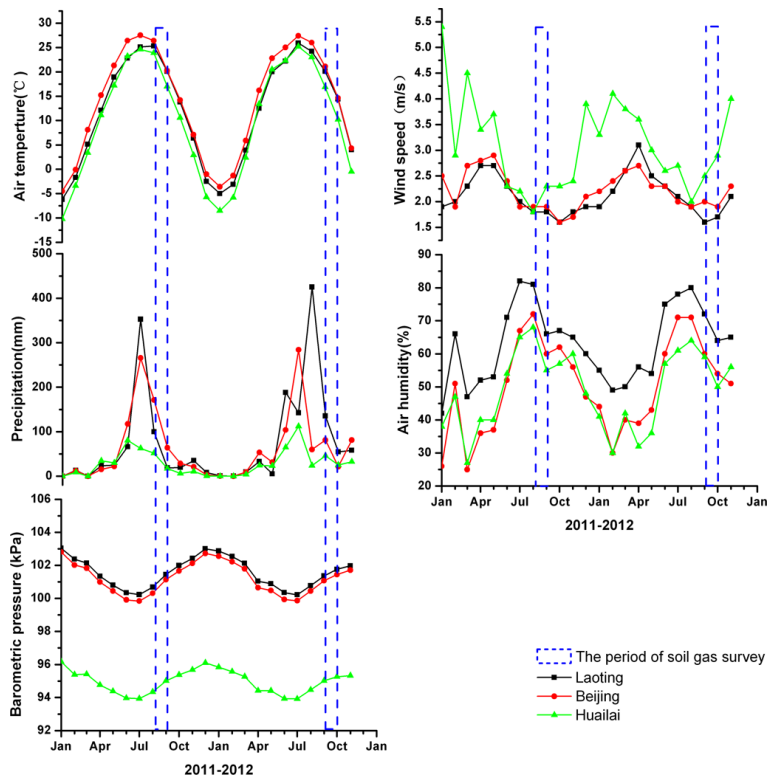


**Fig. 2.** Monthly average values of meteorological parameters in the capital area of China, from January 2011 to November 2012 (China Meteorological Data Sharing Service System). The black lines represent meteorological parameters in Laoting county, Tangshan region; the red lines represent meteorological parameters in Beijing, which is close to Sanhe-Pinggu region; the green lines represent meteorological parameters in Huailai county, Yanqing-Huailai basin; the blue dotted lines represent the period of soil gas surveys.

**Soil gas geochemistry across fault zones**

X. Han et al.

Title Page

Abstract

Introduction

Conclusions

References

Tables

Figures

◀

▶

◀

▶

Back

Close

Full Screen / Esc

Printer-friendly Version

Interactive Discussion



## Soil gas geochemistry across fault zones

X. Han et al.

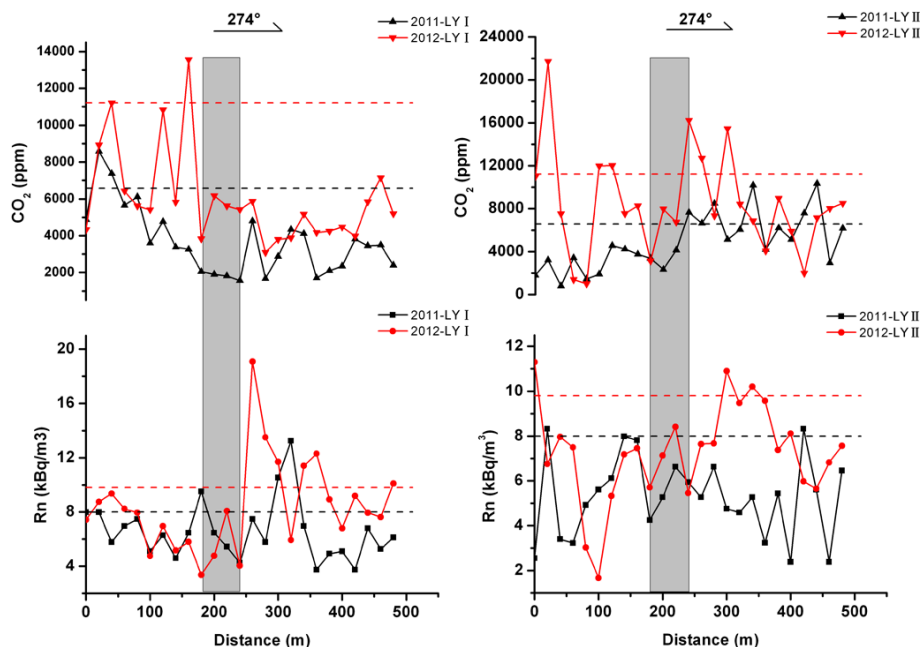


**Fig. 3.** Rn and CO<sub>2</sub> concentrations along LY profile across NEYF Fault. The shaded rectangle represents the location of the fault. The black and red dotted lines represent anomaly threshold of soil gas in 2011 and 2012, respectively.

Title Page

Abstract

Introduction

Conclusions

References

Tables

Figures

◀

▶

◀

▶

Back

Close

Full Screen / Esc

Printer-friendly Version

Interactive Discussion



Soil gas  
geochemistry across  
fault zones

X. Han et al.

Title Page

Abstract

Introduction

Conclusions

References

Tables

Figures

◀

▶

◀

▶

Back

Close

Full Screen / Esc

Printer-friendly Version

Interactive Discussion

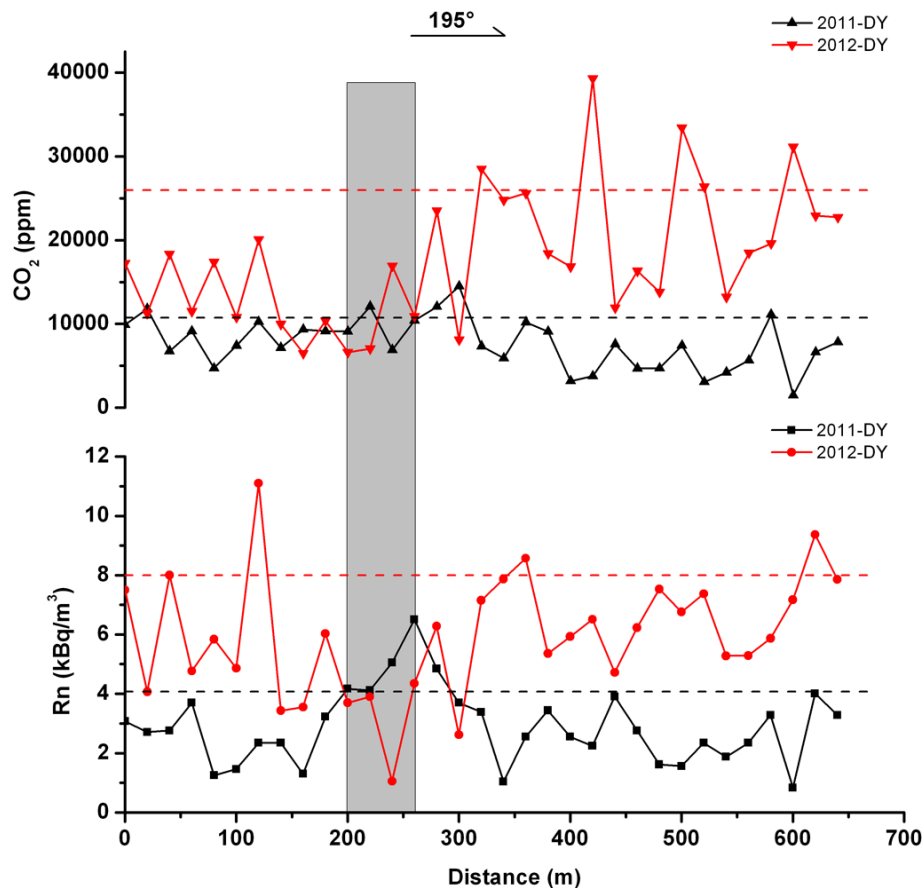


**Fig. 4.** Rn and CO<sub>2</sub> concentrations along DY profile across Xinbaoan-Shacheng Fault. The shaded rectangle represents the location of the fault. The black and red dotted lines represent anomaly threshold of soil gas in 2011 and 2012, respectively.

Soil gas geochemistry across fault zones

X. Han et al.

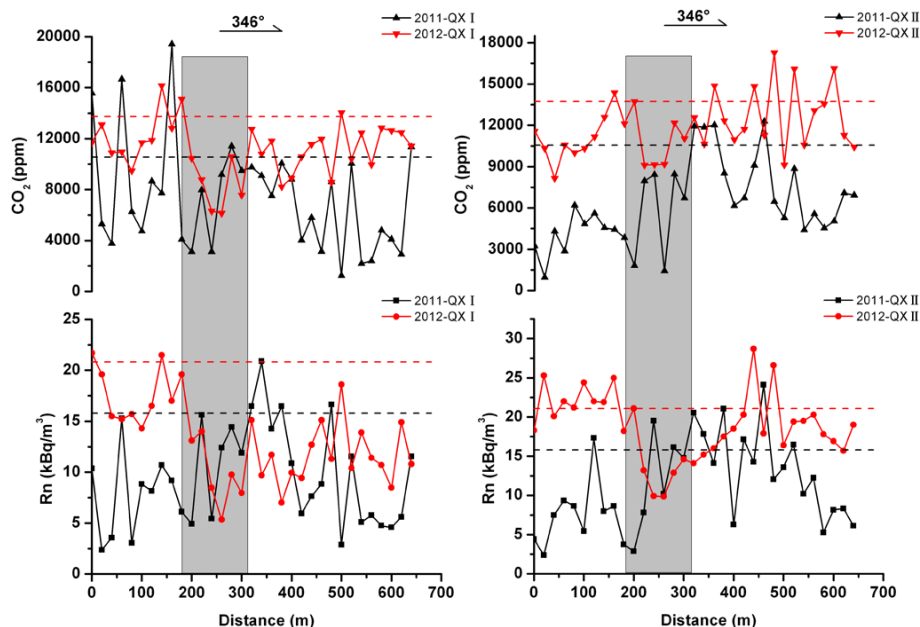


**Fig. 5.** Rn and CO<sub>2</sub> concentrations along QX profile across Xiadian Fault. The shaded rectangle represents the location of the fault. The black and red dotted lines represent anomaly threshold of soil gas in 2011 and 2012, respectively.

Discussion Paper | Discussion Paper | Discussion Paper | Discussion Paper | Discussion Paper

Title Page

Abstract

Introduction

Conclusions

References

Tables

Figures

◀

▶

◀

▶

Back

Close

Full Screen / Esc

Printer-friendly Version

Interactive Discussion



## Soil gas geochemistry across fault zones

X. Han et al.

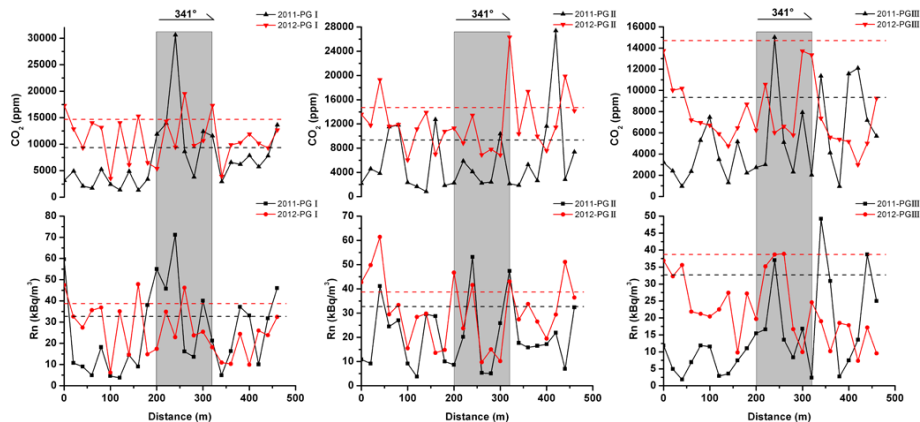


**Fig. 6.** Rn and CO<sub>2</sub> concentrations along PG profile across Xiadian Fault. The shaded rectangle represents the location of the fault. The black and red dotted lines represent anomaly threshold of soil gas in 2011 and 2012, respectively.

Title Page

Abstract

Introduction

Conclusions

References

Tables

Figures

◀

▶

◀

▶

Back

Close

Full Screen / Esc

Printer-friendly Version

Interactive Discussion



Soil gas geochemistry across fault zones

X. Han et al.

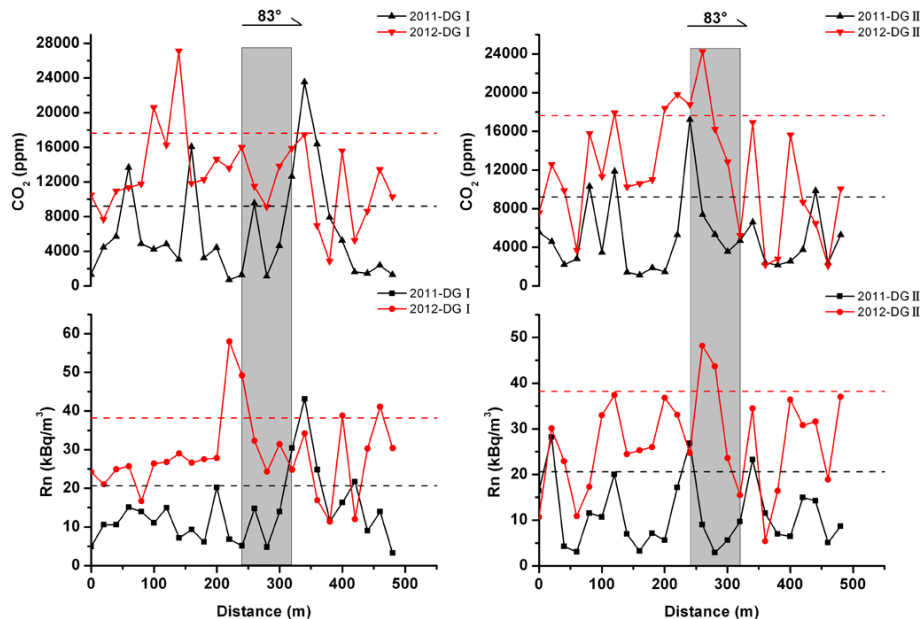


**Fig. 7.** Rn and CO<sub>2</sub> concentrations along DG profile across Xiadian Fault. The shaded rectangle represents the location of the fault. The black and red dotted lines represent anomaly threshold of soil gas in 2011 and 2012, respectively.

Discussion Paper | Discussion Paper | Discussion Paper | Discussion Paper | Discussion Paper

Title Page

Abstract

Introduction

Conclusions

References

Tables

Figures

◀

▶

◀

▶

Back

Close

Full Screen / Esc

Printer-friendly Version

Interactive Discussion



## Soil gas geochemistry across fault zones

X. Han et al.

Title Page

Abstract

Introduction

Conclusions

References

Tables

Figures

◀

▶

◀

▶

Back

Close

Full Screen / Esc

Printer-friendly Version

Interactive Discussion

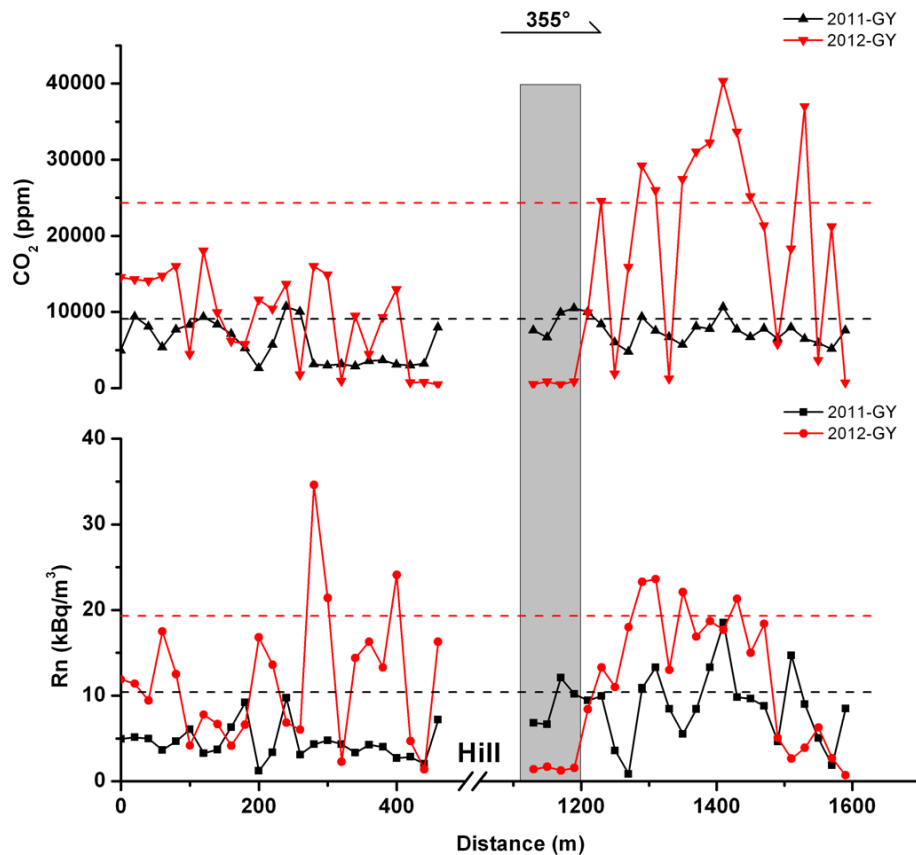


**Fig. 8.** Rn and CO<sub>2</sub> concentrations along GY profile across Tangshan Fault. The shaded rectangle represents the location of the fault. The black and red dotted lines represent anomaly threshold of soil gas in 2011 and 2012, respectively.

Soil gas  
geochemistry across  
fault zones

X. Han et al.

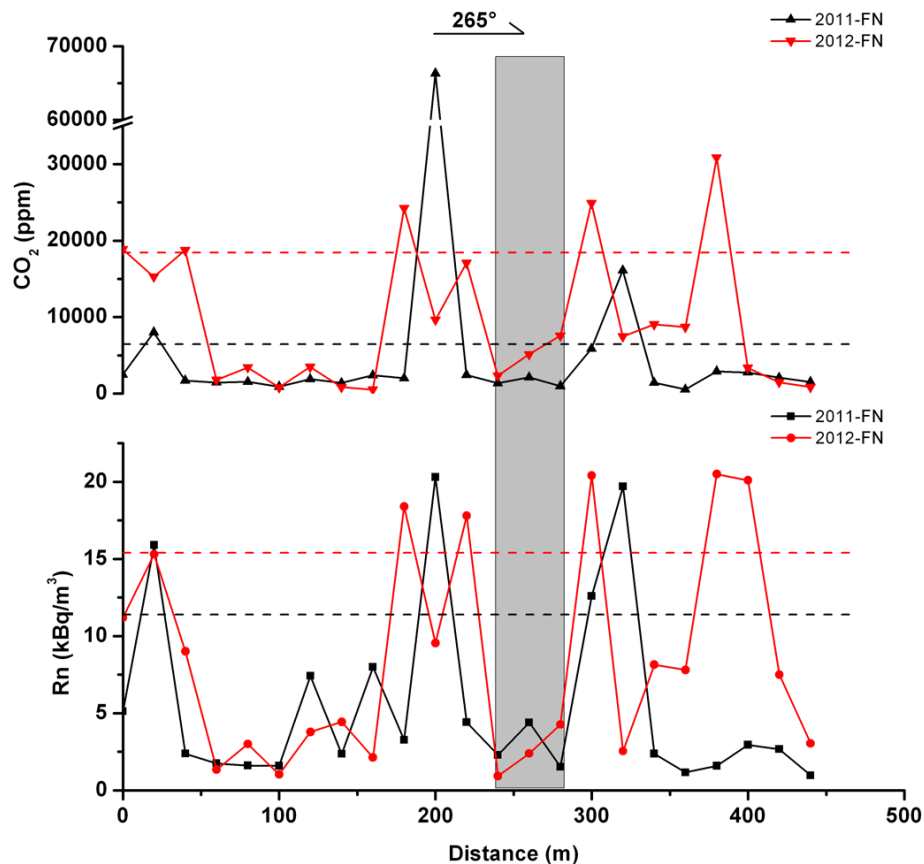


**Fig. 9.** Rn and CO<sub>2</sub> concentrations along FN profile across Tangshan Fault. The shaded rectangle represents the location of the fault. The black and red dotted lines represent anomaly threshold of soil gas in 2011 and 2012, respectively.

Title Page

Abstract

Introduction

Conclusions

References

Tables

Figures

◀

▶

◀

▶

Back

Close

Full Screen / Esc

Printer-friendly Version

Interactive Discussion



## Soil gas geochemistry across fault zones

X. Han et al.

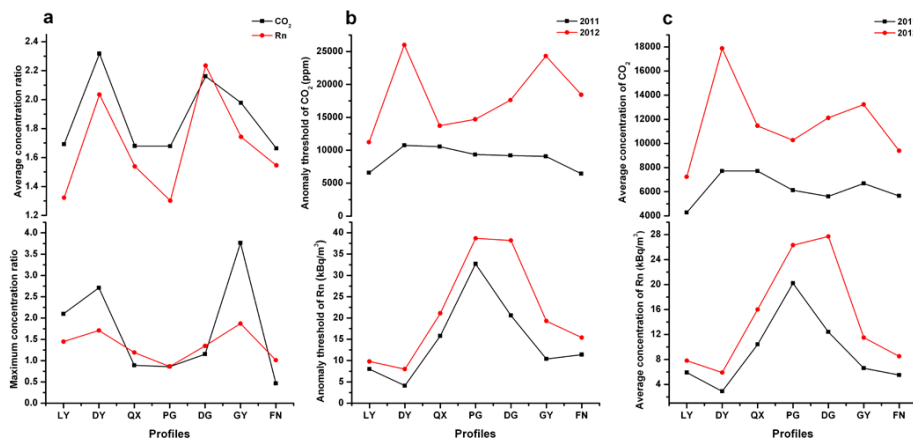


**Fig. 10.** Spatiotemporal variations of soil gases across fault zones in the capital area of China. **(a)** shows the ratios that the average and maximum concentrations of soil gases at one profile in 2012 soil gas survey were divided by that at corresponding profile in 2011 soil gas survey, respectively. **(b)** shows the anomaly thresholds of Rn and CO<sub>2</sub> at different profiles in 2011 and 2012 soil gas surveys. **(c)** shows the average concentrations of Rn and CO<sub>2</sub> at different profiles in 2011 and 2012 soil gas surveys.